ENVIRONMENTAL RESEARCH
LETTERS

LETTER • OPEN ACCESS

Wind turbine wakes can impact down-wind vegetation greenness

To cite this article: Jay E Diffendorfer *et al* 2022 *Environ. Res. Lett.* **17** 104025

IOP Publishing Environ. Res. Lett. 17 (2022) 104025 https://doi.org/10.1088/1748-9326/ac8da9

ENVIRONMENTAL RESEARCH
LETTERS

OPEN ACCESS

RECEIVED
23 May 2022

REVISED
17 August 2022

ACCEPTED FOR PUBLICATION
30 August 2022

PUBLISHED
26 September 2022

LETTER

Wind turbine wakes can impact down-wind vegetation greenness

Jay E Diffendorfer*, Melanie K Vanderhoof and Zach H Ancona

United States Geological Survey, Geosciences and Environmental Change Science Center, Denver, CO 80225, United States of America
* Author to whom any correspondence should be addressed.

E-mail: jediffendorfer@usgs.gov

Keywords: wind energy, vegetation condition, Before After Control Impact, turbine wake, NDVI, Landsat

Supplementary material for this article is available online

Abstract

Global wind energy has expanded 5-fold since 2010 and is predicted to expand another 8–10-fold over the next 30 years. Wakes generated by wind turbines can alter downwind microclimates and potentially downwind vegetation. However, the design of past studies has made it difficult to isolate the impact of wake effects on vegetation from land cover change. We used hourly wind data to model wake and non-wake zones around 17 wind facilities across the U.S. and compared remotely-sensed vegetation greenness in wake and non-wake zones before and after construction. We located sampling sites only in the dominant vegetation type and in areas that were not disturbed before or after construction. We found evidence for wake effects on vegetation greenness at 10 of 17 facilities for portions of, or the entire growing season. Evidence included statistical significance in Before After Control Impact statistical models, differences >3% between expected and observed values of vegetation greenness, and consistent spatial patterns of anomalies in vegetation greenness relative to turbine locations and wind direction. Wakes induced both increases and decreases in vegetation greenness, which may be difficult to predict prior to construction. The magnitude of wake effects depended primarily on precipitation and to a lesser degree aridity. Wake effects did not show trends over time following construction, suggesting the changes impact vegetation greenness within a growing season, but do not accrue over years. Even small changes in vegetation greenness, similar to those found in this study, have been seen to affect higher trophic levels. Given the rapid global growth of wind energy, and the importance of vegetation condition for agriculture, grazing, wildlife, and carbon storage, understanding how wakes from wind turbines impact vegetation is essential to exploit or ameliorate these effects.

1. Introduction

Wind energy is rapidly and globally expanding, having increased at a rate of ∼21% a year since 2010 with forecasts of a ∼10-fold increase in installed capacity by 2050 as many countries implement policies supporting increased renewable energy (International Renewable Energy Agency 2019, International Energy Agency 2021). Continued growth of wind energy, however, has technical (Veers *et al* 2019), social (Mai *et al* 2021) and environmental hurdles (Katzner *et al* 2019) to overcome. Widely acknowledged environmental impacts include wildlife deaths from turbine collisions, habitat loss, and behavioural avoidance of wind facilities by some species (Allison *et al* 2019). A newly emerging, potential environmental impact may be the effects of turbine wakes ('wakes') on microclimates and vegetation. Wind turbines generate wakes as they remove energy from wind resulting in lower wind speeds and increased turbulence. These wakes are large enough to reduce energy generation at downwind facilities (Lundquist *et al* 2019). They can also change air, surface, and soil temperatures, as well as humidity (Zhou *et al* 2012, Armstrong *et al* 2016, Xia *et al* 2016, Rajewski *et al* 2020), but not always (Moravec *et al* 2018). Field-collected and remotely-sensed surface temperature data show wakes can cause nighttime warming up to 1.5 °C–1.9 °C (Rajewski *et al* 2013, Smith *et al* 2013) and cool daytime

temperatures (Rajewski *et al* 2013, Xia *et al* 2016), although these effects vary with wind conditions and season.

A small number of studies suggest wakes may impact vegetation. Kaffine (2019) found US counties with larger capacities of installed wind energy had larger crop yields, but this study did not identify underlying mechanisms. Several studies have used remote sensing to investigate wind energy impacts on vegetation greenness. One reported no effects (Xia and Zhou 2017), one reported increased greenness (Luo *et al* 2021), and one reported a decrease in greenness and leaf area index (Tang *et al* 2017). In addition, a recent, comprehensive study found increased, decreased, and no changes to vegetation greenness across 319 wind facilities in the US (Qin *et al* 2022).

These studies, however, were not designed to separate changes in vegetation caused by surface disturbance from those caused by wakes. For example, all four studies used 300 m to 1 km resolution satellite imagery, so the pixels included a mix of vegetation, roads, buildings, and agriculture. In addition, changes in vegetation were analysed across all pixels in the study extent, including those pixels disturbed by the installation of the facility, as well as pixels experiencing ongoing 'background' levels of land cover change or agriculture. Of those papers finding changes in vegetation greenness, two papers describe land cover change as the main mechanism (Luo *et al* 2021, Qin *et al* 2022), not wake effects. Furthermore, these studies used distance buffers to estimate wake and no wake zones, instead of modelled wakes based on wind direction, which limited their ability to isolate microclimate impacts on vegetation.

Several studies have shown that the installation of wind energy results in surface disturbance, but that the area impacted by surface disturbance is small relative to the general size of the facility (Denholm *et al* 2009, Diffendorfer *et al* 2019). If wakes, not surface disturbance, alter vegetation condition, then wind facilities have the potential to affect a much larger area than that initially impacted by construction activities. In this study, we designed a sampling strategy to control for vegetation change caused by site construction and isolate the effects of wakes from turbines on vegetation greenness. Our focus on wake effects, not surface disturbance, is unique relative to previous studies on vegetation change at wind facilities.

Because atmospheric conditions like air temperature are fundamental drivers of plant growth, we hypothesized that wakes could affect vegetation greenness. However, effects may be subtle because wake impacts on microclimates might occur only in specific wind regimes, at certain times, and in proximity to turbines. Wake impacts on biological processes may therefore occur seasonally and be variable across wind facilities, depending on the interaction between local wind regimes, weather, the layout of the turbines, and the plant community. Quantifying potential microclimate effects on vegetation greenness caused by turbine wakes requires a methodology that uses wind direction to identify wake and non-wake locations while also controlling for the potential influence of land cover change.

We investigated the impact of wakes on vegetation greenness at 17 wind facilities across the United States representing diverse vegetation types (figure 1(a), supplementary table S1). Vegetation greenness was measured using 30 m resolution Normalized Difference Vegetation Index (NDVI) from Landsat. Impacts were evaluated across different time periods in the growing season and periods of high versus low precipitation. We used a Before After Control Impact (BACI) statistical design to compare vegetation greenness before and after construction in wake (impact) and no or low wake (control) zones. Wake and control zones were delineated by applying Jensen's wake decay model and hourly wind direction data ((Gelaro *et al* 2017), supplementary figure S1 and table S2) from the year of construction to 2019 at each turbine (figure 1(c)) and predicting the cumulative, interactive wake effect from all turbines out to 10 km at each facility (figure 1(d)). We randomly selected 200 sampling points in each wake and control zone, only sampling pixels representing the dominant vegetation class, not classified as pasture (to avoid grazing effects), or cultivated crops, and those that did not change land cover type before and after facility construction based on the National Land Cover Database (NLCD) (2001–2016, figure 1(e)). Sampling points reduces potential bias attributable to spatial autocorrelation relative to analysing a continuous surface (Ives *et al* 2021). To test for evidence of wake effects on greenness at each facility we: (1) performed BACI analyses using linear mixed effects models to determine if wakes impacted NDVI. (2) Calculated the change in wake NDVI relative to expected, using the before and after control NDVI. (3) Mapped the spatial patterns of wake impacts on greenness. And (4) developed secondary linear mixed effects models to investigate variables driving the magnitude of wake effects on greenness.

2. Method

We describe below the following components of our approach: (1) Selecting wind facilities across the US that varied in natural vegetation and geographic region. (2) Characterizing vegetation phenology at each facility to determine the optimal time periods for sampling NDVI. (3) Modelling wake and low-wake zones using hourly wind data. (4) Controlling for land use change in the sample locations and allocating sampling 'points' across wake and low-wake zones. (5) Processing the remotely-sensed vegetation greenness data before and after construction at each

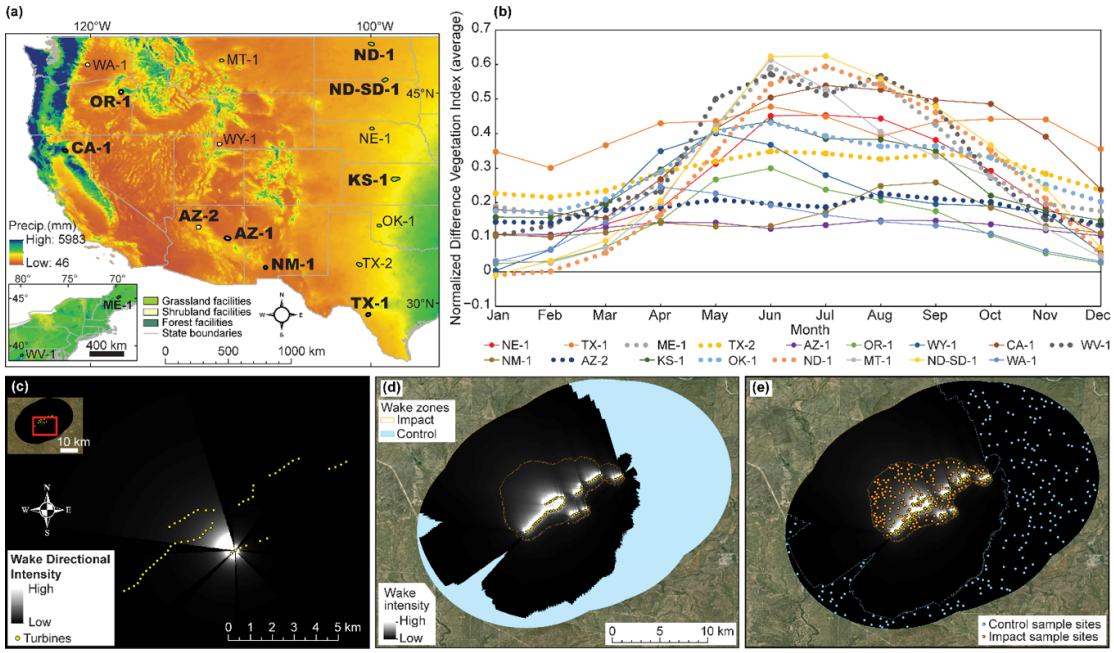

Figure 1. Wake zone modelling and sampling at facilities. 17 wind facility locations with the ten facilities showing evidence for wake effects on greennes in bold (a), average NDVI for each facility used to determine peak, up and down time periods (b), single wind turbine wake modelled using Jensen's decay formula (c), combined interacting wakes with control and impact areas defined by wake intensity (d), sample points in control and wake zones (e).

facility. (6) Analysing the vegetation greenness data using a BACI statistical design. (7) Modelling the drivers of vegetation anomalies within the wake zones after construction.

2.1. Wind facility selection

The potential impact of wind facilities on vegetation greenness was evaluated across 17 wind facilities in the US (supplementary table S1). Using the United States Wind Turbine Database (USWTDB, Rand *et al* 2020), we selected facilities based on multiple factors. First, we chose facilities isolated from others (>20 km) to assure wake effects came from a single wind facility. Second, because we wanted to detect potential trends in vegetation through time after construction, we selected facilities installed prior to 2016, allowing a minimum of 4 years of post-construction data. The USWTDB includes the year a facility became operational, often called the year of commissioning, though we use 'construction or post-construction'. Third, wake effects may differ across climate regimes and vegetation communities, so we selected facilities dominated by shrubland, grassland, or forest land cover classes and representing a broad spatial coverage of the US (except for the southeast due to a lack of facilities). Fourth, we focused on utility scale turbines 1.5 MW or greater in nameplate capacity.

2.2. Vegetation phenology and sample timing

We estimated the timing of seasonal vegetation growth at each facility using all pixels within a Minimum Convex Polygon (MCP) created around the turbine locations at a facility. We selected all pixels within the MCP corresponding to the dominant 'natural' vegetation type using the 2016 NLCD (30 m resolution). Doing so excluded urban, agriculture, water, and other non-vegetation cover types. We derived a pre-construction vegetation phenology by averaging 8–16-day NDVI data to a single value per month across all pixels in the MCP for 5 years pre-construction. NDVI values were derived from Landsat 5, 7, and 8 surface reflectance image collections in Google Earth Engine.

For each facility, we used the average annual phenological pattern of NDVI to demarcate three periods of the growing season (figure 1(b)). The 3 months with the highest NDVI were 'peak greenness', and these months did not have to be continuous. The 'green up' period was the two months preceding the first month of peak greenness and the 'green down' period was the two months following the final month of peak greenness (supplementary table S1). We filtered the data by monthly precipitation to generate the high (upper 25th percentile) and low (lower 25th percentile) precipitation periods. We also analysed the data across the entire growing season.

2.3. Modelling turbine wakes

A key part of detecting wake effects is determining 'control' locations where turbine wakes are absent or minimal. These areas should share similar weather and vegetation composition as the wake zones. We identified wake and 'non wake' areas by integrating hourly wind direction and distance from turbines with Jensen's wake model (Jensen 1983), to estimate the proportional decline in wake velocity

from each turbine individually, and then summing these declines across all turbines.

Modelling turbine wakes included four primary steps. First, we summarized hourly wind direction from the year of installation to 2019 for eight wind directions (NNE, ENE, ESE, SSE, SSW, WSW, WNW, NNW) up to 10 kilometres from each turbine. We used wind direction data from the Modern-Era Retrospective analysis for Research and Applications (MERRA-2, (Gelaro *et al* 2017)). MERRA-2 is a widely used meteorological dataset, and many studies have investigated how biases in wind speed in MERRA2 (and other climate reanalyses) may affect estimates of wind energy power output (Gruber *et al* 2019, Jourdier 2020, Gualtieri 2022). Perhaps because wind direction does not factor into power production, far fewer analyses exist for wind direction. Carvalho (2019) show MERRA2 wind direction estimates have relatively low bias, and lower than other modern reanalyses in the US, though they are measured with uncertainty. Similar results were found in Pakistan (Asim *et al* 2020).

The MERRA-2 data include U-wind (eastward) and V-wind (northward) components representing the wind velocity every hour at 50 m above surface. We converted hourly U and V wind vectors into direction in R (R Core Team 2018) and calculated the proportion of hours wind occurred in each of the 8 wind direction classes (supplementary figure 1 and table S2). For example, if a facility had 8 years of post-construction data and a 3 month growing season each year and there were 1728 h in the NE wind direction, then 10% of the hourly data were in the NE direction because (8 years $\times$ 3 months $\times$ 30 d $\times$ 24 h = 17 280 total hours and 1728/17 280 = 0.1).

Second, within any one of the 8 wind directions, we had multiple hourly observations of wind. We used the mean and 1.5 standard deviations of these hourly data to generate the mean direction and outward spread of the wake from each turbine, resulting in a binary raster map of where the wake occurred within each of the 8 direction classes. The value of the pixel was the proportion of the total hours wind occurred in that wind direction.

Third, for each turbine, we generated a distance raster map, where each pixel represented the distance from the turbine. From this, we calculated the proportional decline in velocity using Jensen's model. Jensen's wake formulation models velocity at a distance downwind from a turbine:

$$v = u\left\{1 - {}^{2}/_{3}\left(\frac{r_o}{r_o - \propto x}\right)^{2}\right\} \quad (1)$$

where r_o is the rotor diameter, u is the wind velocity entering the turbine, x is distance, and α is the decay constant,

$$\propto = \frac{0.5}{\ln\left({}^{z}/_{z_o}\right)} \quad (2)$$

where z is the hub height and z_o is the surface roughness. Following Shakoor *et al* (2016), we set z_o to 0.075 and retrieved z from the USWTDB. Given the goal of using an easily generalizable approach that adequately modelled where the majority of wake effects occur at a facility, we did not attempt more refined approaches that might include different surface roughness values based on the surrounding land cover.

In equation (1), dividing both sides by u results in the proportional decline in velocity and makes the right-hand side of Jensen's equation independent of wind speed. We used this formulation to estimate the proportional decline in velocity at different distances from wind turbines of specific hub heights. This generated a raster map for each turbine that was the modelled proportional decline in velocity from the turbine.

Fourth, for each turbine we multiplied the proportional decline in velocity with the proportion of hours wind occurred in a given direction, effectively weighting the proportional decline in velocity by the proportion of time wind came from that direction (figure 1(c)). We then summed the wake direction/decay maps across all turbines to create a single 'wake effect' map for each facility (figure 1(d)). We note the single turbine wake model did not explicitly include the effects of one turbine on another and the loss of energy to downwind turbines from upwind turbines. Our approach may be improved by more complex wake modelling.

Turbine wake effect maps had many pixels with very small wake effect values, and far fewer with larger modelled wake effects (figure 1(d)). Given these right-skewed distributions, we used a geometric classification in ArcGIS 10.6 to delineate 4 'wake zones'. The skewed nature of the data meant the differences between the low wake effect zones (3 and 4) were small. To assure our sampling locations were stratified across areas with and without potential wake effects, we used zone 4 as 'controls' and combined zones 1 and 2 into a 'wake zone'. Zone 3 was reclassified as a buffer between the wake zone and control zone and no locations in this zone were sampled (figure 1(d)).

2.4. Sampling strategy- land cover change and sample allocation

Sampling was designed as a BACI study. We selected sampling points at each wind facility in wake and low-wake (control) zones that met specific land cover criteria. Previous studies of wake effects used remotely-sensed temperature or vegetation data that did not exclude land cover change. To avoid sampling land cover change, we used four versions of NLCD data (2001, 2006, 2011 and 2016) to filter pixels that only included the dominant vegetation type at the facility

and excluded pixels that changed from one land cover type to another at any interval from 2001 to 2016. For grassland and shrubland facilities, if a dominant land-cover type was present (i.e. either grassland or shrubland) a single land cover type was used. If the site contained a mix of grassland and shrubland, these were combined into a single class due to the NLCD's low accuracy in distinguishing these two land cover types from one another (Chen *et al* 2005). For forested facilities, we manually checked NLCD categories using high resolution aerial photography in Google Earth Pro at our sampling points (see next paragraph). We determined the misclassification rate between forest and mixed forest was too large to separate these two classes with confidence, so we combined them.

We randomly generated 200 sampling points within each wake and low-wake zone (400 total points per facility, figure 1(e)) in ArcGIS 10.6.1. Sampling points were $\geqslant$150 m apart to minimize spatial autocorrelation. A visual inspection of each sample point was conducted using high resolution imagery to confirm each sample and the surrounding 90 m^2 was fully within the dominant vegetation class and did not sample the edge of an impervious surface or a different land cover type; when necessary, the sampling point was moved away from edges into the dominant vegetation class.

2.5. Remotely-sensed data

Landsat NDVI values were analysed as a surrogate of vegetation greenness (Tucker 1979). NDVI is the most widely used spectral index of vegetation greenness (Lawley *et al* 2016). NDVI was selected over the Enhanced Vegetation Index, as low leaf area index was more common across facilities than high leaf area index and associated potential NDVI saturation. Landsat Thematic Mapper and Enhanced Thematic Mapper images were converted to surface reflectance using the Landsat Ecosystem Disturbance Adaptive Processing System algorithm (Masek *et al* 2006). Landsat Operational Land Imager images were converted to surface reflectance using the Landsat Surface Reflectance Code algorithm (Vermote *et al* 2016). Values identified as cloud or cloud shadow were masked using cFMask (Foga *et al* 2017). All cloud-free NDVI observations over the identified growing season, from 5 years pre-construction through 2019, were consolidated into consecutive 8 d periods and exported from Google Earth Engine. Erroneous values can still persist, attributable to a subset of images having a higher root mean square error, errors in converting raw images to surface reflectance, poor or uneven atmospheric conditions, or residual cloud or cloud shadows (Masek *et al* 2006, Feng *et al* 2012). To minimize inclusion of potentially erroneous observations, all NDVI observations $\leqslant$=0 or >0.99 were assumed to be erroneous and removed (1.6% of observations). Further, time series of NDVI were graphed and extreme outliers were identified and removed (0.2% of observations).

2.6. Before-After-Control-Impact analyses

We followed statistical approaches for BACI studies with multiple, paired, sampling events before and after the treatment (Underwood 1994). Low-wake zones were considered controls. Treatment (control vs wake) and period (before vs after construction) were fixed effects. Sampling points were modelled as random effects and to capture monthly variation in NDVI that varied from year to year, monthly NDVI was a random effect nested within year. Data within the year of construction were excluded because we did not know when the facility began operating within the year. We ran the linear mixed effects models in R using lmer in the lme4 package (Bates *et al* 2015).

We focused on the treatment by period interaction, which determines if any changes in NDVI before and after construction were different between wake and no-wake zones. This isolates potential wake effects from other background changes such as a long-term increase or decrease in overall vegetation greenness across the entire study area. This 'BACI contrast' was estimated from the model expected marginal means as (CA–CB)–(WA–WB), where CA = control zone, after construction; CB = control zone, before construction; WA = wake zone, after construction; and WB = wake zone, before construction. We also compared random effects only models to fixed effects models, as well as models with main effects only (treatment and period) to models with main effects and the BACI contrast (treatment by period). Models were compared using sample size adjusted Akaike's information criterion (AICc) to check for evidence that models with fixed effects and the BACI contrast had greater support than random effects models.

BACI analyses were performed across 6 'time periods': the entire growing seasons (All months) and data filtered to periods of green up (spring), peak greenness, green down (late summer to fall), and high and low precipitation.

We used multiple lines of evidence to determine if turbine wakes affected vegetation greenness. First, if the BACI contrasts were not statistically significant at $p \leqslant 0.05$, we concluded evidence for wake effects was not sufficient. The BACI statistical models had large sample sizes and hence they estimated small BACI contrasts as statistically significant at $p \leqslant 0.05$. If the BACI contrasts were significant at $p \leqslant 0.05$ we then evaluated the magnitude of the effect. The BACI contrasts varied considerably in size depending on the dominant vegetation type. Arid regions had very low baseline NDVI values with BACI contrasts much lower than forested locations, so we could not simply use the size of the BACI contrast as an estimate of effect size. Instead, we calculated an expected mean NDVI in wake zones after construction and compared it to the observed mean NDVI. If wakes

had no impact on NDVI, we would expect wake and control zones to change identically through time such that $WA/WB = CA/CB$. The expected NDVI in wake zones ($WA_{expected}$) was simply the mean NDVI in wake zones before construction (WB) multiplied by the ratio of the mean NDVI in control zones after and before construction:

$$WA_{expected} = WB \times \frac{CA}{CB} \quad (3)$$

We then calculated the percent change between the observed (WA) and expected NDVI in wake zones after construction:

$$Change\ relative\ to\ expected = 100 \times \frac{(WA - WA_{expected})}{WA_{expected}} \quad (4)$$

Cases where the BACI contrast was statistically significant at $p \leqslant 0.05$ and the change relative to expected was greater than 3% were considered evidence for an effect. We used these admittedly subjective thresholds to assure transparency in the methods. Others may select a less stringent p-value and/or a different value for change relative to expected. To visualize the results and further confirm the BACI results, we compared the statistical outputs to time series graphs of monthly mean NDVI values for control and wake zones as well as maps of the change in NDVI before vs after construction across all 17 facilities using data across the entire growing season (the 'All Months' time period, figure 4). For these maps, we first calculated the difference between a sampling point vs the mean NDVI value across all control points for each month and calculated the mean anomaly across months. We then subtracted the mean of these monthly anomalies after construction from the mean before construction. We mapped these differences in relation to turbine locations and the modelled wake zones.

2.7. Drivers of wake effects

The BACI analyses modelled the interactive effects of wakes and pre vs post installation on vegetation greenness but did not allow a more refined understanding of how wake effects might respond to explanatory variables that change through time and across space. To understand these more nuanced patterns, we modelled the anomaly in NDVI during the entire growing season for the four facilities showing consistent wake effects across all time periods (AZ-1, CA-1, NM-1, and TX-1). At these facilities, we used just those samples within the wake zone, after the year of construction, and calculated the anomaly in NDVI at each point in the wake zone, for each month, by subtracting the mean NDVI across all control points at the month of interest from each point in the wake zone (figures 2(c) and (d), mean anomaly time series).

For each facility, we fit a set of linear mixed effects models to the post construction, monthly NDVI anomaly, using a set of covariates that could drive wake effects on greenness. Topographic covariates were derived from the U.S. Geological Survey Digital Elevation Model at 30 m resolution (Gesch *et al* 2018), and included the (1) percent slope, (2) distance to nearest turbine (m), (3) change in elevation between each sampling point and the nearest turbine, and (4) folded aspect. Aspect measures the direction a slope faces and influences solar radiation intensity and heat load, which affects plant community composition and growth. Following McCune and Keon (2002), folded aspect provides higher values for slopes with a SW aspect:

$$Aspect_{folded} = abs\,(180 - abs\,(aspect - 225)) \quad (5)$$

We derived climate covariates from the Parameter-elevation Regressions on Independent Slopes Model (PRISM, monthly, 4 km resolution, (Daly *et al* 2008)). Four of the covariates were calculated as anomalies from the climate normal (1981–2010): (1) maximum temperature from June to August (°C), (2) maximum vapour pressure deficit (VPD) from June to August (hPa), (3) annual precipitation (mm), and (4) the 3 months, cumulative lagged precipitation. Aridity and the 3 months cumulative lagged aridity were also included as covariates. Aridity was calculated as the monthly ratio of precipitation and potential evapotranspiration (PET). PET indicates the atmospheric demand for evaporation and transpiration in the absence of water limitations and was calculated from PRISM and North American Land Data Assimilation System Phase 2 datasets using minimum and maximum temperature, daily average dew point temperature (equivalently, vapour pressure or VPD), wind speed, and downward shortwave radiation (Mitchell *et al* 2004, Abatzoglou 2013). All these climate covariates can affect plant growth and thus potentially influence how wake effects impact vegetation greenness.

The models also included an annual linear trend. Each sample, month, and year were included as random variables with months nested within year. The model set included all additive combinations of the covariates but to avoid multicollinearity we did not include covariates with correlations $\geqslant$0.6 in the same model.

We ranked the set of models using AICc, interpreted as the conditional probability that a model is the best model in the candidate model set. We used model-averaged standardized coefficients and their standard errors (Galipaud *et al* 2017) and the relative variable importance (Giam and Olden 2016) to determine which covariates were the most important across the candidate model set. Model-averaged standardized coefficients, were calculated using all models in the candidate model set, substituting zero

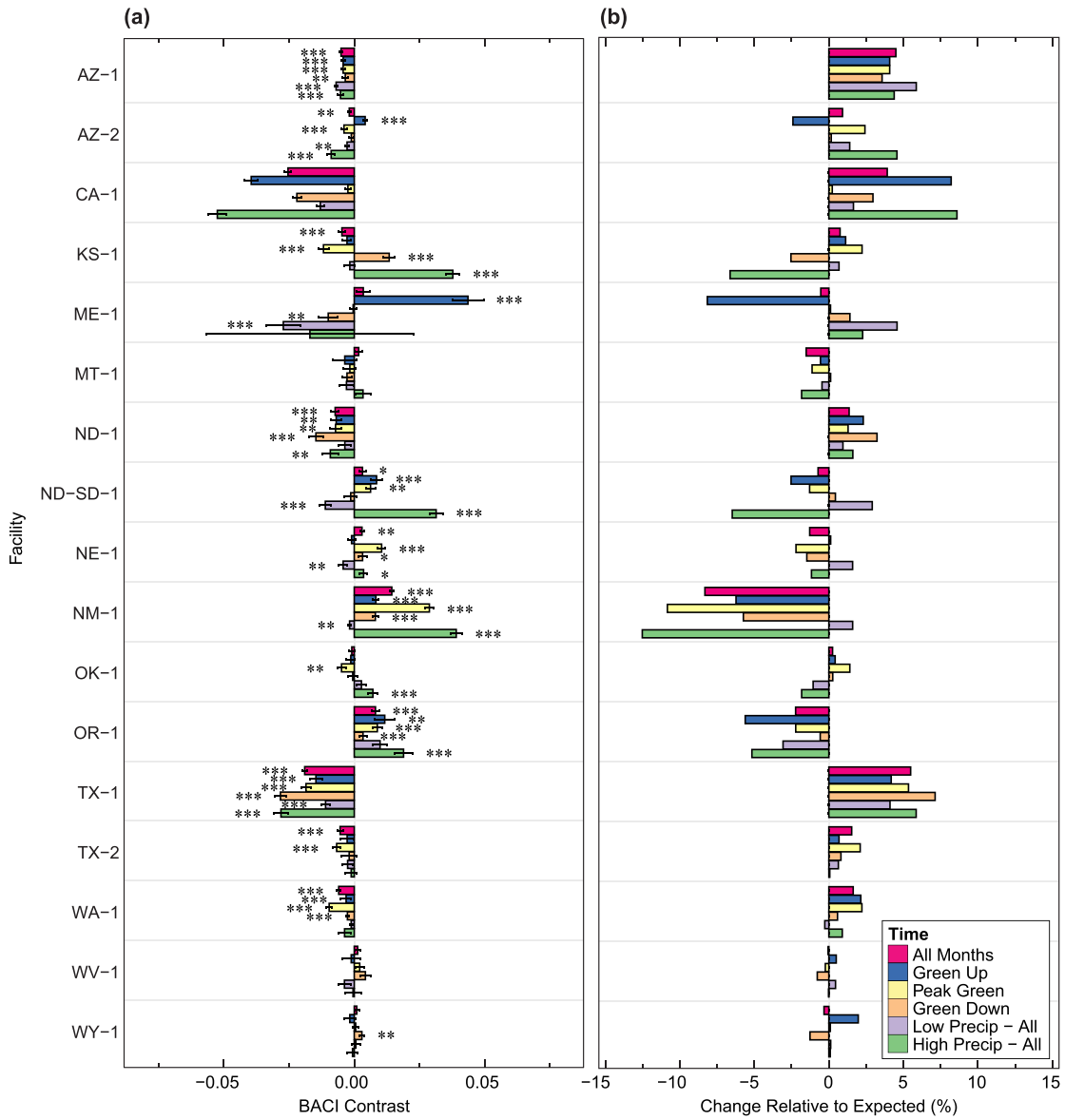

Figure 2. BACI contrasts (a) and their levels of statistical significance ($^{*}p \leqslant 0.05$, $^{**}p \leqslant 0.01$, $^{***}p \leqslant 0.001$) and change relative to expected difference in NDVI (b) for each facility and time period.

when the parameter of interest was absent (Burnham and Anderson 2002).

To estimate model coefficients and effect sizes we calculated the unstandardized model-averaged estimates and their standard errors because full model-averaged estimates can produce biased estimates of effect sizes (Grueber *et al* 2011, Symonds and Moussalli 2011). Finally, we generated biplots of the anomaly in NDVI versus the covariate of interest while setting the other covariates at their mean values to understand patterns in the response and visually check the modelled relationship. For both the BACI and anomaly analyses we calculated a pseudo-R^2 value (Nakagawa *et al* 2017) to estimate the variance explained by fixed effects in the models.

All the covariate data used in the analyses are publicly available (supplementary table S6). All analyses were performed in R 4.1.1 (R Core Team 2018).

3. Results

10 of 17 wind facilities showed evidence for wake effects on greenness during one or more time periods (AZ-1, AZ-2, CA-1, KS-1, ME-1, ND-1, ND-SD-1, NM-1, OR-1, TX-1, figures 2(a) and (b), supplementary table S3). Evidence for wake effects was defined as: statistically significant BACI interaction terms and a change in wake zone NDVI relative to expected of $\geqslant$3% post-construction. Times series graphs of NDVI or the anomaly in NDVI across the BACI contrasts (figures 3(a) and (b)), and spatial patterns in the NDVI anomaly post-construction derived from data across the entire growing season were consistent with the statistical models (figures 4(a) and (b)). We illustrate these visual lines of evidence with the four facilities that had the largest change relative to expected in NDVI across the majority or all time periods

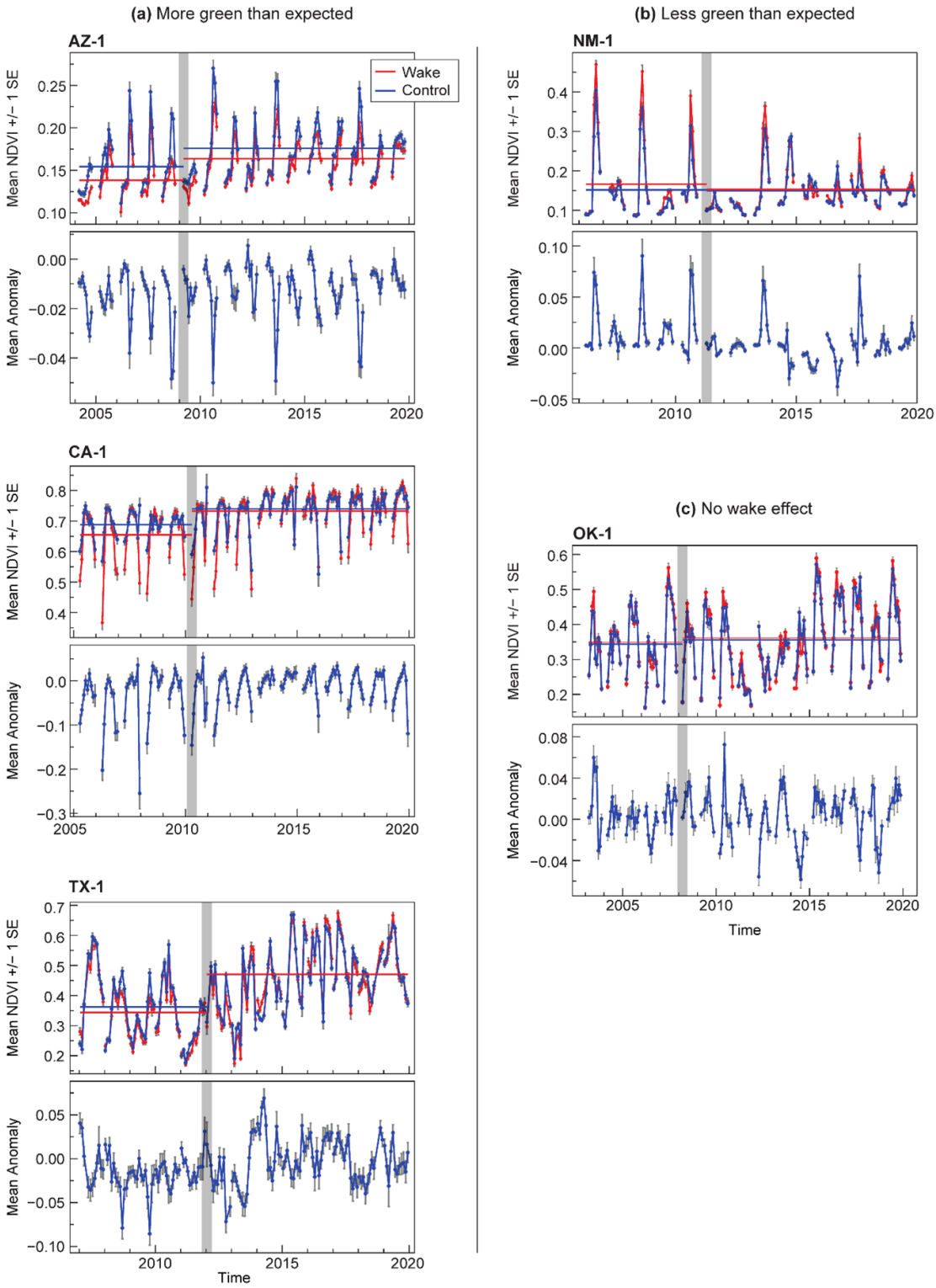

Figure 3. Time series of either NDVI (wake = red, control = blue), or mean anomaly in NDVI between control and wake zones for the five facilities with wake effects across most time periods. (a) shows three facilities that had increases in NDVI, (b) shows decreases in NDVI, and (e) shows no change in NDVI. The time series show data across the entire growing season, though the effect size of wakes on vegetation were larger in other time periods in some cases.

(AZ-1, CA-1, NM-1, TX-1, figure 2(b)). These facilities had visual evidence for wake effects (figures 3(a) and (b), figures 4(a) and (b)), while facilities without wake effects on vegetation consistently showed little or no evidence in time series or maps (figures 3(c) and 4(c)).

At the ten facilities with wake effects on vegetation, we observed both increases and decreases in greenness with the change relative to expected in wake zones ranging from −12.5% to 8.6% (figure 2(b), supplementary table S3). At KS-1, ME-1, ND-SD-1, NM-1, and OR-1 wake zones were less green than

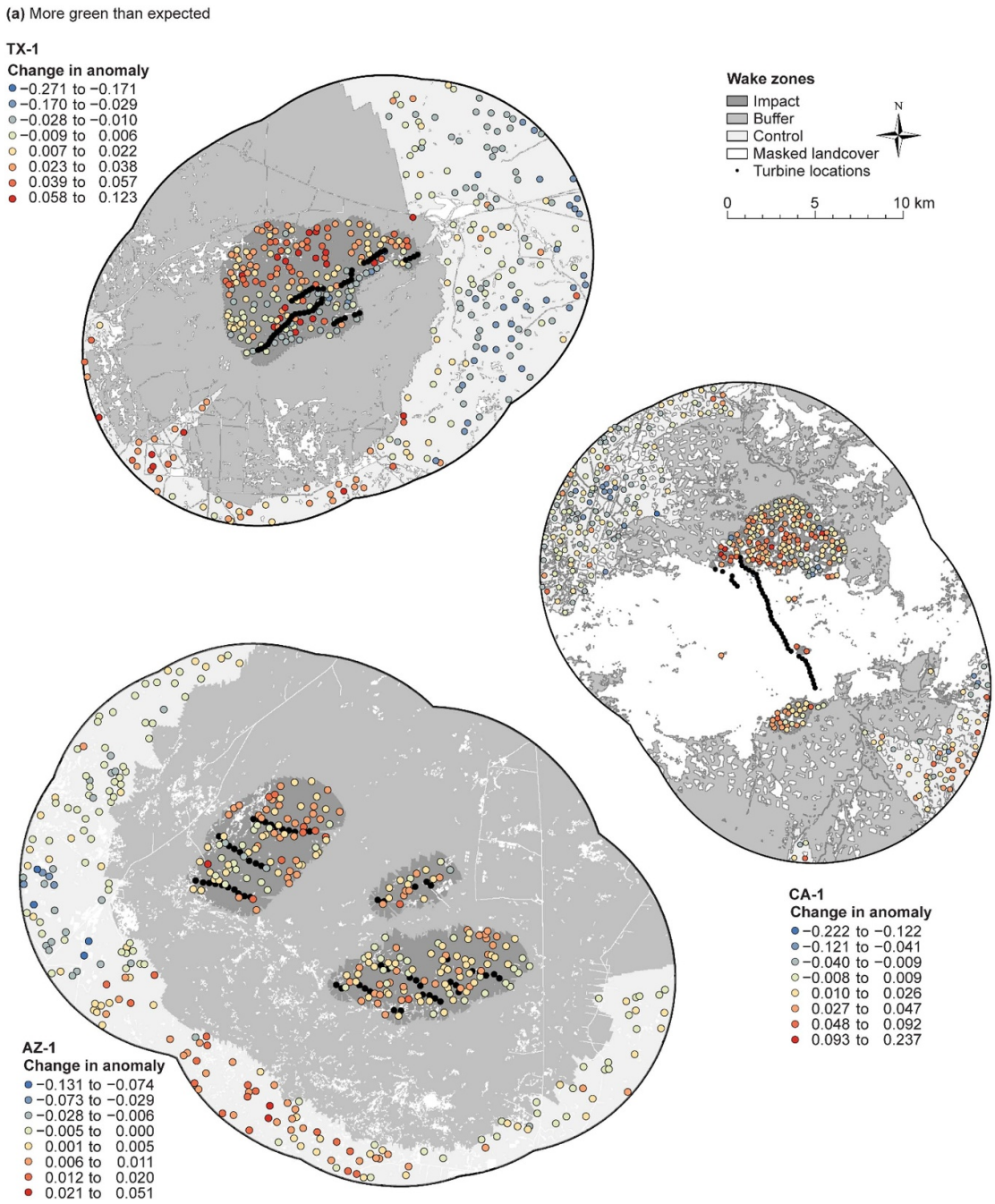

Figure 4. Maps of the difference (before—after construction) of the mean anomaly at each sampling point in the study. Maps illustrating mean NDVI anomaly at sampling points in Control (light gray) and wake zones (dark gray) for five facilities with wake effects across most time periods. The maps show data across the entire growing season, though the effect size of wakes on vegetation were larger in other time periods in some cases. OK-1 is included as a facility showing no wake effects.

expected while at AZ-1, AZ-2, CA-1, ND-1, and TX-1 wake zones were greener than expected during all or some time periods. At ME-1, wake effects increased vegetation greenness during green up but decreased it during periods of low precipitation (figures 2(a) and (b)). Qualitatively, facility characteristics such as dominant vegetation or region (supplementary table S1) were not associated with the direction of wake effects.

Maps of the post construction anomaly in NDVI across the entire growing season were generally consistent with BACI contrasts (figure 4) but also show underlying patterns of spatial variability. At TX-1 and NM-1 (figures 4(a) and (b)) patterns of anomalies were highly consistent with wake effects. TX-1 had the largest anomalies at sampling points downwind from turbines based on wind direction (supplementary figure 1) while NM-1 had the largest anomalies within the turbine arrays and to the north. At AZ-1, and CA-1 (figure 4(a)), spatial patterns were not as distinct, but sampling points in wake zones generally had larger anomalies in NDVI than

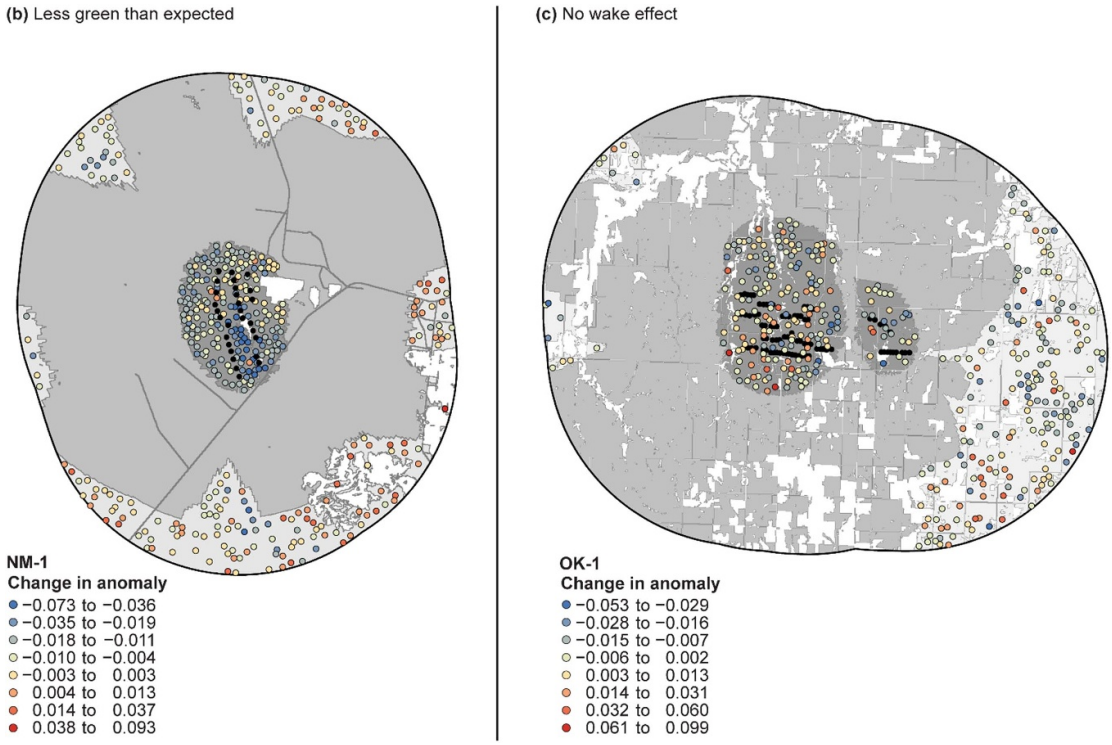

Figure 4. (Continued.)

control points, especially compared to OK-1 (no wake effect, figure 4(c)), though considerable variation in the anomalies occurred within both wake and control zones.

Across the four facilities showing wake effects throughout all months of the growing season, climate variables associated with plant growth were the most common factors explaining spatial and temporal variability in the magnitude of the wake zone greenness anomaly (figure 5, supplementary tables S4 and S5). The fixed effects (i.e. topographic, climatic, and facility explanatory variables in these models explained 25%–51% of the variation in the greenness anomaly (supplementary table S4). Precipitation (lagged or current) had high relative variable importance and model averaged standardized coefficients at all four facilities; the anomaly in NDVI increased with increasing precipitation at NM-1 and TX-1 and declined with increasing precipitation at the other facilities (figure 5, supplementary table S4). Aridity, lagged aridity, anomaly in temperature, and anomaly in maximum VPD explained variation in wake anomaly at some facilities. Physical characteristics had few impacts on the wake anomaly, with distance to nearest turbine affecting the anomaly at only one facility (TX-1). At all facilities, year, as a linear trend, had low relative variable importance, consistent with the time series plots (figures 3(a) and (b)), suggesting anomalies did not increase or decrease through time after construction.

4. Discussion

Our results provide strong evidence that the wakes generated by wind facilities, independent of land cover change, can affect vegetation greenness, as measured by NDVI. We also illustrate nuances in these effects, which occurred at some facilities but not others, and varied in magnitude and the directional change in greenness. Wake effects also varied by the time of year and the climatic variables associated with plant growth. The conditions under which wake effects impact vegetation are not easily predicted. Wind facilities in shrublands, forests, grasslands, and on ridgetops or flat ground all showed wake effects and facilities with no wake effects similarly spanned several land cover types.

Wakes both increased and decreased vegetation greenness and the lack of multi-year trends in the magnitude of NDVI anomalies suggested wake effects on vegetation are confined within a growing season, or even part of a growing season. Further research is needed to disentangle whether a change in NDVI represents a change in leaf condition (i.e. stress or moisture), leaf cover, or a shift in herbaceous species composition, all of which influence gross primary productivity.

Precipitation was a dominant variable influencing the magnitude of wake-induced changes in greenness. While moisture availability is a primary driver of plant productivity, the response of vegetation to

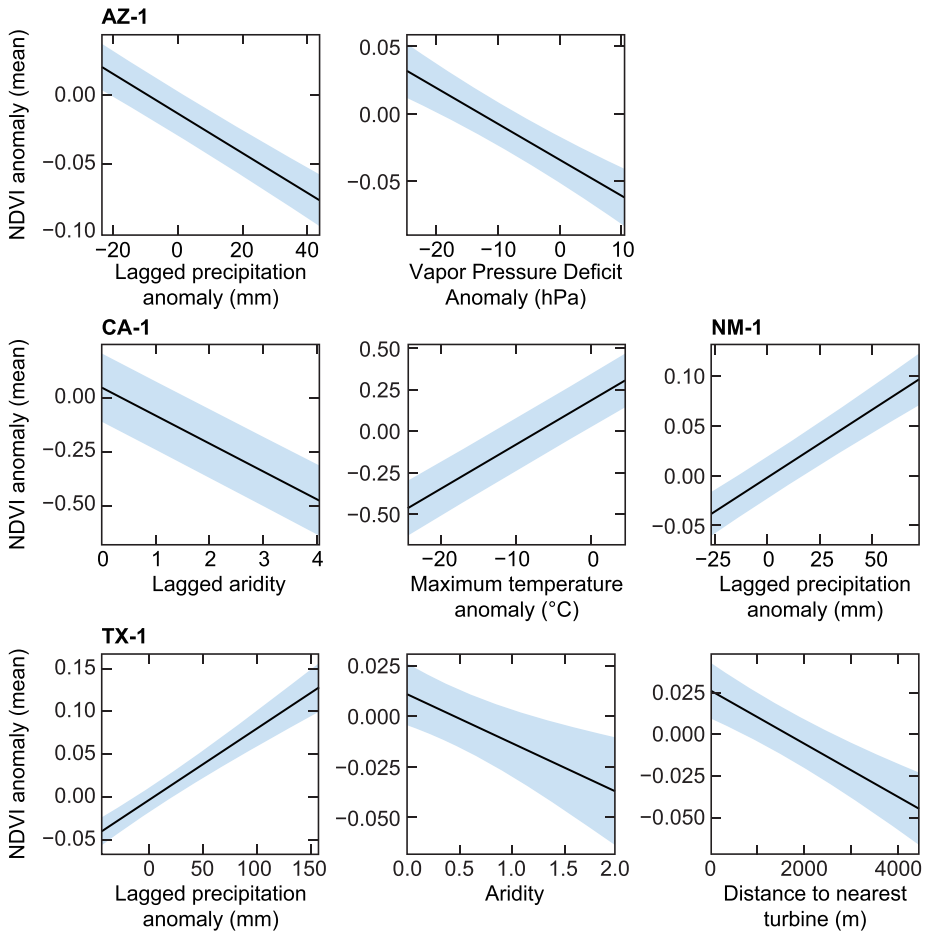

Figure 5. Biplots of the anomaly in NDVI vs explanatory variables. Plots for five facilities with wake effects across most time periods. Light blue bands show 95% confidence intervals, and the black line is the predicted value from the linear mixed effects model holding all other covariates at their mean values.

changing moisture will depend on the antecedent conditions, or the water status of the plant community and soil, so both increasing and decreasing greenness in response to wakes is a reasonable finding. Aridity and VPD were also consistently identified as important variables. We suggest wake-induced changes in microclimate modify the response of NDVI to precipitation by influencing surface evaporation, stomatal resistance, and plant evapotranspiration. Agricultural wind breaks show similar site-dependent effects on vegetation, with both directionality and magnitude of the change in greenness varying by year (Cleugh 1998). The stability of wind entering a facility, its upstream moisture profile, the configuration of turbines, and the degree of mixing caused by turbines can all influence downwind patterns of humidity (Adkins and Sescu 2022), suggesting existing atmospheric conditions, design aspects of the wind facility, and the underlying plant community might all interact to determine if wakes impact vegetation.

Our observed changes in NDVI were small compared to processes such as wildfire or land conversion that entirely alter vegetation communities. However, because NDVI reflects primary productivity, biomass, and vegetation structure and condition, even relatively small changes in NDVI have been linked to changes in ecological systems and habitat condition. For example, increases in NDVI on overwintering grounds of 0.05 were associated with changes in clutch size from 4 to 4.5 in barn swallows (López Calderón *et al* 2019), and statistical models relating NDVI to mule deer density in the western US suggest changes in NDVI of 0.02 can alter density by ∼33 animals/100 km^2 (Stoner *et al* 2018). Finally, species richness, abundance, and biomass, as well as the seasonal phenology of insects have been linked to NDVI (Rhodes *et al* 2022). For example, in Australia ground dwelling beetle species richness and abundance increased by ∼15% and 25% respectively for every 0.1 increase in NDVI (Lassau and Hochuli 2008). At CA-1, KS-1, ME-1, ND-SD-1, NM-1, and TX-1, BACI contrasts suggest changes in mean NDVI were $\geqslant$∼0.03 during one or more of the time periods we measured, suggesting wake effects on vegetation may be 'biologically meaningful', with repercussions for consumers and higher trophic levels. Some of our arid sites (AZ-1, and NM-1) had low NDVI

values (∼0.12–0.19) and small BACI contrasts during some time periods, yet a substantial percent change in NDVI relative to expected (AZ-1 = 3.6%–5.9%, NM-1 = − 5.7 to −12.5%). In arid systems, even small changes in NDVI may result in large relative deviations from baseline conditions, but it remains unknown how proportional changes in NDVI translate to direct impacts on consumers at wind facilities.

Ecological studies at terrestrial wind energy facilities show a variety of responses (including no response) to wind facilities (Schuster *et al* 2015, Allison *et al* 2019, Coppes *et al* 2020). To our knowledge, ecological studies relating wake induced microclimate impacts to vegetation change and higher trophic levels have not yet been done.

Using an approach that isolated microclimate from land cover change, we found wind wakes impacted down-wind vegetation greenness at ∼60% of the wind facilities we studied and that some of these changes may be large enough to impact ecological processes. This suggests impacts from wind energy may go beyond direct land transformation from roads and turbine pads. It also suggests previous studies on wind energy impacts on vegetation greenness may have measured microclimate effects caused by wakes on vegetation alongside impacts from land cover change. 14 of our 17 wind facilities were also examined by Qin *et al* (2022). Though not a direct comparison, we checked Qin *et al*'s (2022) peak greenness NDVI anomaly at the closest wake buffer, vs our anomaly at peak greenness. While four of the 14 facilities showed negative anomalies in both studies and two showed positive anomalies, the remaining eight showed different directions of change. We suggest these differences are primarily caused by land cover change processes occurring in Qin's study that were excluded from consideration in this study. This suggests the methodological approach used in wake effect studies is critical when isolating wake effects and measuring effect sizes. More studies are required to understand the best methods for analysing wake effects, but our approach used high resolution imagery, controlled for land cover change, only focused on the dominant vegetation class, visually verified that sampling points were properly located, and explicitly modelled wake zones.

5. Conclusion

Previous studies of wind energy impacts on vegetation greenness had limited ability to distinguish if observed changes were caused by the installation of, and ongoing landcover change around, the facility or by the wakes caused by turbines. We designed an approach that distinguished wake and non-wake zones using simple wake models and hourly wind direction. We also controlled for land cover change by removing pixels that changed and targeting the dominant vegetation type at each facility. We showed wakes from wind turbines, independent of land transformation, can impact vegetation greenness.

Wakes induced increased or decreased vegetation greenness at ten of 17 facilities based on BACI analyses, maps of the anomaly in greenness and the difference between expected and observed greenness in wake zones. While the observed changes in NDVI were relatively small, in some cases the change in greenness were of a magnitude previously documented to affect ecological processes such as clutch size, population abundance, and species richness. The magnitude of wake effects depended primarily on precipitation and to a lesser degree aridity. Future research should advance spatial modelling of predicted wake zones, improve our ability to predict the directionality of the wake impact, and concurrently track microclimate, vegetation, and other ecological variables.

As wind energy expands rapidly and globally, further consideration of its potential positive and negative impacts to both natural and managed vegetation will be critical for agricultural and grazing productivity, habitat condition, and carbon storage, all of which co-exist with wind facilities. For example, if we understand the conditions resulting in positive wake effects on vegetation it may help us place turbines in locations creating 'win-wins' for energy production and perhaps increased agricultural yields or carbon sequestration. Understanding where negative wake effects occur can help predict necessary operational, siting, or management actions to lessen such impacts. As in offshore environments, where wakes affect surface wave energy and the water column (van Berkel *et al* 2020, Bärfuss *et al* 2021), we are just beginning to understand how wakes from wind turbines impact the terrestrial environment and if we can exploit their positive benefits and ameliorate any negative effects.

Data availability statement

The data that support the findings of this study are openly available at the following URL/DOI: https://doi.org/10.5066/P9P3J7GR. Data will be available from 30 September 2022.

Acknowledgments

We thank M Huso and W Thogmartin for their insights on statistical and coding issues, and C Schwarz for making his BACI R code publicly available. J Lindquist and her lab provided a wonderful discussion on wake modelling and data sources. J Havens assisted with the graphics. L Lopez-Hoffman, S Loss, and B Straw provided a pre-submission review of the manuscript. L Kramer conducted a final check of the data and code to verify its completeness and functionality. Funding for the

research came from the Land Change Science Program at USGS. Any use of trade, firm, or product names is for descriptive purposes only and does not imply endorsement by the U.S. Government.

ORCID iDs

Jay E Diffendorfer https://orcid.org/0000-0003-1093-6948
Melanie K Vanderhoof https://orcid.org/0000-0002-0101-5533
Zach H Ancona https://orcid.org/0000-0001-5430-0218

References

Abatzoglou J T 2013 Development of gridded surface meteorological data for ecological applications and modelling *Int. J. Climatol.* **33** 121–31
Adkins K A and Sescu A 2022 Wind farms and humidity *Energies* **15** 2603
Allison T D *et al* 2019 Impacts to wildlife of wind energy siting and operation in the United States *Issues Ecol.* **23** D07S90
Armstrong A, Burton R R, Lee S E, Mobbs S, Ostle N, Smith V, Waldron S and Whitaker J 2016 Ground-level climate at a peatland wind farm in Scotland is affected by wind turbine operation *Environ. Res. Lett.* **11** 044024
Asim M, Hussain A, Uddin G M, Hayat N and Qureshi F I 2020 Comparing MERRA and MERRA-2 reanalysis datasets with mast measured wind data for Karachi, Pakistan *Pak. J. Eng. Appl. Sci.* **26** 55–62
Bärfuss K, Schulz-Stellenfleth J and Lampert A 2021 The impact of offshore wind farms on sea state demonstrated by airborne LiDAR measurements *J. Mar. Sci. Eng.* **9** 644
Bates D, Mächler M, Bolker B and Walker S 2015 Fitting linear mixed-effects models using lme4 *J. Stat. Softw.* **67** 1–48
Burnham K P and Anderson D R 2002 *Model Selection and Multimodel Inference: A Practical Information-theoretic Approach* (New York: Springer-Verlag))
Carvalho D 2019 An assessment of NASA's GMAO MERRA-2 reanalysis surface winds *J. Clim.* **32** 8261–81
Chen P-Y, Luzio M D and Arnold J G 2005 Spatial assessment of two widely used land-cover datasets over the continental U.S *IEEE Trans. Geosci. Remote Sens.* **43** 2396–404
Cleugh H A 1998 Effects of windbreaks on airflow, microclimates and crop yields *Agrofor. Syst.* **41** 55–84
Coppes J, Braunisch V, Bollmann K, Storch I, Mollet P, Grünschachner-Berger V, Taubmann J, Suchant R and Nopp-Mayr U 2020 The impact of wind energy facilities on grouse: a systematic review *J. Ornithol.* **161** 1–15
Daly C, Halbleib M, Smith J I, Gibson W P, Doggett M K, Taylor G H, Curtis J and Pasteris P P 2008 Physiographically sensitive mapping of climatological temperature and precipitation across the conterminous United States *Int. J. Climatol.* **28** 2031–64
Denholm P, Hand M, Jackson M and Ong S 2009 Land-use requirements of modern wind power plants in the United States *NREL/TP-6A2-4 5834 (National Renewable Energy Laboratory)* (available at: www.nrel.gov/docs/fy09osti/45834.pdf)
Diffendorfer J E, Dorning M A, Keen J R, Kramer L A and Taylor R V 2019 Geographic context affects the landscape change and fragmentation caused by wind energy facilities *PeerJ* **7** e7129
Feng M, Huang C, Channan S, Vermote E F, Masek J G and Townshend J R 2012 Quality assessment of Landsat surface reflectance products using MODIS data *Comput. Geosci.* **38** 9–22
Foga S, Scaramuzza P L, Guo S, Zhu Z, Dilley R D, Beckmann T, Schmidt G L, Dwyer J L, Joseph Hughes M and Laue B 2017 Cloud detection algorithm comparison and validation for operational Landsat data products *Remote Sens. Environ.* **194** 379–90
Galipaud M, Gillingham M and Dechaume-Moncharmont X-F 2017 A farewell to the sum of Akaike weights: the benefits of alternative metrics for variable importance estimations in model selection *Methods Ecol. Evol.* **8** 1668–78
Gelaro R *et al* 2017 The Modern-Era Retrospective Analysis for Research and Applications, Version 2 MERRA-2 *J. Clim.* **30** 5419–54
Gesch D B, Evans G A, Oimoen M J and Arundel S 2018 The national elevation dataset (American Society for Photogrammetry and Remote Sensing) pp 83–110 (available at: http://pubs.er.usgs.gov/publication/70201572)
Giam X and Olden J D 2016 Quantifying variable importance in a multimodel inference framework *Methods Ecol. Evol.* **7** 388–97
Gruber K, Klöckl C, Regner P, Baumgartner J and Schmidt J 2019 Assessing the global wind atlas and local measurements for bias correction of wind power generation simulated from MERRA-2 *Brazil Energy* **189** 116212
Grueber C E, Nakagawa S, Laws R J and Jamieson I G 2011 Multimodel inference in ecology and evolution: challenges and solutions *J. Evol. Biol.* **24** 699–711
Gualtieri G 2022 Analysing the uncertainties of reanalysis data used for wind resource assessment: a critical review *Renew. Sustain. Energy Rev.* **167** 112741
International Energy Agency 2021 *2021 World Energy Outlook* (Paris: International Energy Agency) (available at: www.iea.org/reports/world-energy-outlook-2021)
International Renewable Energy Agency 2019 *Future of Wind: Deployment, Investment, Technology, Grid Integration and Socio-Economic Aspects (A Global Energy Transformation Paper)* (Abu Dhabi: International Renewable Energy Agency)
Ives A R, Zhu L, Wang F, Zhu J, Morrow C J and Radeloff V C 2021 Statistical inference for trends in spatiotemporal data *Remote Sens. Environ.* **266** 112678
Jensen N O 1983 *A Note on Wind Generator Interaction* Riso-M No. 2411 (Riso National Laboratory) (available at: https://backend.orbit.dtu.dk/ws/files/55857682/ris_m_2411.pdf)
Jourdier B 2020 Evaluation of ERA5, MERRA-2, COSMO-REA6, NEWA and AROME to simulate wind power production over France advances in *Science and Research 19th EMS Annual Meeting: European Conf. for Applied Meteorology and Climatology 2019*— vol 17 (Copernicus GmbH) pp 63–77 (available at: https://asr.copernicus.org/articles/17/63/2020/)
Kaffine D T 2019 Microclimate effects of wind farms on local crop yields *J. Environ. Econ. Manage.* **96** 159–73
Katzner T E *et al* 2019 Wind energy: an ecological challenge *Science* **366** 1206–7
Lassau S A and Hochuli D F 2008 Testing predictions of beetle community patterns derived empirically using remote sensing *Divers. Distrib.* **14** 138–47
Lawley V, Lewis M, Clarke K and Ostendorf B 2016 Site-based and remote sensing methods for monitoring indicators of vegetation condition: an Australian review *Ecol. Indic.* **60** 1273–83
López Calderón C, Balbontín Arenas J, Hobson K A and Møller A P 2019 Age-dependent carry-over effects in a long-distance migratory bird *Sci. Rep.* **9** 12032
Lundquist J K, DuVivier K K, Kaffine D and Tomaszewski J M 2019 Costs and consequences of wind turbine wake effects arising from uncoordinated wind energy development *Nat. Energy* **4** 26
Luo L, Zhuang Y, Duan Q, Dong L, Yu Y, Liu Y, Chen K and Gao X 2021 Local climatic and environmental effects of an onshore wind farm in North China *Agric. For. Meteorol.* **308–309** 108607

Mai T, Lopez A, Mowers M and Lantz E 2021 Interactions of wind energy project siting, wind resource potential, and the evolution of the U.S *Power Syst. Energy* **223** 119998

Masek J G, Vermote E F, Saleous N E, Wolfe R, Hall F G, Huemmrich K F, Gao F, Kutler J and Lim T-K 2006 A Landsat surface reflectance dataset for North America, 1990–2000 *IEEE Geosci. Remote Sens. Lett.* **3** 68–72

McCune B and Keon D 2002 Equations for potential annual direct incident radiation and heat load *J. Veg. Sci.* **13** 603–6

Mitchell K E *et al* 2004 The multi-institution North American land data assimilation system (NLDAS): utilizing multiple GCIP products and partners in a continental distributed hydrological modeling system *J. Geophys. Res.* **109** D07S90

Moravec D, Barták V, Puš V and Wild J 2018 Wind turbine impact on near-ground air temperature *Renew. Energy* **123** 627–33

Nakagawa S, Johnson P C D and Schielzeth H 2017 The coefficient of determination R2 and intra-class correlation coefficient from generalized linear mixed-effects models revisited and expanded *J. R. Soc. Interface* **14** 20170213

Qin Y, Li Y, Xu R, Hou C, Armstrong A, Bach E, Wang Y and Fu B 2022 Impacts of 319 wind farms on surface temperature and vegetation in the United States *Environ. Res. Lett.* **17** 024026

R Core Team 2018 *R: A Language and Environment for Statistical Computing* (Vienna: R Foundation for Statistical Computing) (available at: www.R-project.org)

Rajewski D A *et al* 2013 Crop wind energy experiment (CWEX): observations of surface-layer, boundary layer, and mesoscale interactions with a wind farm *Bull. Am. Meteorol. Soc.* **94** 655–72

Rajewski D A, Takle E S, VanLoocke A and Purdy S L 2020 Observations show that wind farms substantially modify the atmospheric boundary layer thermal stratification transition in the early evening *Geophys. Res. Lett.* **47** e2019GL086010

Rand J T, Kramer L A, Garrity C P, Hoen B D, Diffendorfer J E, Hunt H E and Spears M 2020 A continuously updated, geospatially rectified database of utility-scale wind turbines in the United States *Sci. Data* **7** 1–12

Rhodes M W, Bennie J J, Spalding A, Ffrench-constant R H and Maclean I M D 2022 Recent advances in the remote sensing of insects *Biol. Rev.* **97** 343–60

Schuster E, Bulling L and Köppel J 2015 Consolidating the state of knowledge: a synoptical review of wind energy's wildlife effects *Environ. Manage.* **56** 300–31

Shakoor R, Hassan M, Raheem A and Wu Y 2016 Wake effect modeling: a review of wind farm layout optimization using Jensen's model *Renew. Sustain. Energy Rev.* **58** 1048–59

Smith C M, Barthelmie R J and Pryor S C 2013 *In situ* observations of the influence of a large onshore wind farm on near-surface temperature, turbulence intensity and wind speed profiles *Environ. Res. Lett.* **8** 034006

Stoner D C, Sexton J O, Choate D M, Nagol J, Bernales H H, Sims S A, Ironside K E, Longshore K M and Edwards Jr TC 2018 Climatically driven changes in primary production propagate through trophic levels *Glob. Change Biol.* **24** 4453–63

Symonds M R E and Moussalli A 2011 A brief guide to model selection, multimodel inference and model averaging in behavioural ecology using Akaike's information criterion *Behav. Ecol. Sociobiol.* **65** 13–21

Tang B, Wu D, Zhao X, Zhou T, Zhao W and Wei H 2017 The observed impacts of wind farms on local vegetation growth in Northern China *Remote Sens.* **9** 332

Tucker C J 1979 Red and photographic infrared linear combinations for monitoring vegetation *Remote Sens. Environ.* **8** 127–50

Underwood A J 1994 On beyond BACI: sampling designs that might reliably detect environmental disturbances *Ecol. Appl.* **4** 3–15

van Berkel J, Burchard H, Christensen A, Mortensen L O, Petersen O S and Thomsen F 2020 The effects of offshore wind farms on hydrodynamics and implications for fishes *Oceanography* **33** 108–17

Veers P *et al* 2019 Grand challenges in the science of wind energy *Science* **366** eaau2027

Vermote E, Justice C, Claverie M and Franch B 2016 Preliminary analysis of the performance of the landsat 8/OLI land surface reflectance product *Remote Sens. Environ.* **185** 46–56

Xia G and Zhou L 2017 Detecting wind farm impacts on local vegetation growth in Texas and Illinois using MODIS vegetation greenness measurements *Remote Sens.* **9** 698

Xia G, Zhou L, Freedman J M, Roy S B, Harris R A and Cervarich M C 2016 A case study of effects of atmospheric boundary layer turbulence, wind speed, and stability on wind farm induced temperature changes using observations from a field campaign *Clim. Dyn.* **46** 2179–96

Zhou L, Tian Y, Baidya Roy S, Thorncroft C, Bosart L F and Hu Y 2012 Impacts of wind farms on land surface temperature *Nat. Clim. Change* **2** 539–43